Journal of Applied Mechanics and Technical Physics, Vol. 35, No. 1, 1994

DISCRETE NONLINEAR-DISPERSION SHALLOW-WATER MODEL

A. M. Frank

UDC 532.59

The discrete approach to the formulation of numerical continuum mechanics models has recently expanded significantly. Following the first works [1, 2], there appeared discrete gasdynamic, magnetohydrodynamic, ideal compressible fluid, and deformable solid models, utilizing the fundamental conservation laws with any number of degrees of freedom. These models are basically formulated for quite general cases of medium motion, and in the incompressible fluid case, for example, they are the discrete analogs of the complete Euler equations. An exception is [3], in which a discrete nonlinear shallow-water model without dispersion is formulated. For the two-dimensional discrete incompressible fluid model, proposed in [4], in the calculation of solitary waves on a coarse mesh there was noted its definite similarity with the nonlinear-dispersion shallow-water models. The study of the dispersion relationship of this model for the problem of linear waves in a fluid of finite depth showed that by selecting the mesh parameters we can control in wide limits the dispersion properties of the model, obtaining both the exact law $\omega^2 = k\tanh(k)$ in the limit as the mesh spacing $h \to 0$ and a law very close to $\omega^2 = k^2/(1 + k^2/3)$ for moderate values of h. Thus the model of [4] is an example of a discrete mathematical model, which with the use of detailed spatial discretization is the finite-dimensional analog of the complete Euler equations, and with the use of coarser discretization is the analog of the nonlinear-dispersion shallow-water equations. However, it is found that in the framework of this discrete approach we can directly formulate a simpler nonlinear-dispersion shallow-water model, which, just as in the continuum case, has lower dimensionality and therefore is more convenient and economical in the modeling of long waves.

1. Equations of Motion. We shall examine the problem of long gravitational wave motion in an inviscid incompressible fluid above a nonplane bottom. We break the fluid layer into the elementary liquid volumes V_i (Fig. 1). In accordance with the conventional concepts in shallow-water theory, we shall consider that the fluid velocity component parallel to the bottom varies weakly with depth, and by virtue of the continuity equation the velocity component normal to the bottom varies with depth from zero to some value at the surface, following a nearly linear law. With this distribution of the velocities the shear deformation of the volumes V_i is not large, and therefore we can try to describe this flow as the motion of an ensemble of volumes V_i, each of which is examined as a material particle, traveling without friction along the bottom and having the mass $m_i = \rho V_i$ and two degrees of freedom; ξ_i is the coordinate along the curve describing the bottom relief, and σ_i is the characteristic thickness of the fluid layer along the normal to the bottom. We write the kinetic energy of this system with account for the foregoing assumptions approximately in the form

$$T = \frac{1}{2}\sum_i m_i(\dot{\xi}_i^2 + \alpha\dot{\sigma}_i^2), \tag{1.1}$$

where α is a coefficient that arises upon integrating the square of the fluid velocity component normal to the bottom through the volume V_i, equal to 1/3 in the case of linear variation of this velocity component along the normal.

For tracking the position of the free boundary it is convenient to introduce the special nonmaterial marker-particles S_i (Fig. 1) with the Cartesian coordinates x_i and y_i. Then we represent the potential energy of the discrete system similarly to [4] as

$$\Pi = \int_\Omega\int \rho g y dx dy. \tag{1.2}$$

Krasnoyarsk. Translated from Prikladnaya Mekhhanika i Tekhnicheskaya Fizika, No. 1, pp. 34-42, January-February, 1994. Original article submitted March 2, 1993.

0021-8944/94/3501-0034$12.50

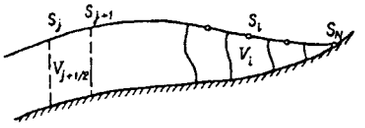

Fig. 1

Here ρ is the fluid density; g is the free-fall acceleration; Ω is the region occupied by the fluid if we take the broken line drawn through S_i as the free boundary. It is clear that Π depends on the coordinates of the markers and that this relationship is easily calculated in explicit form. Thus, in the case of a channel with vertical side walls we have

$$\Pi = \Pi_0 + \frac{\rho g}{6} \sum_{i=1}^{N-1} (x_{i+1} - x_i)\,(y_i^2 + y_i y_{i+1} + y_{i+1}^2),$$

where Π_0 depends only on the choice of the Cartesian coordinate system origin.

It is also convenient to introduce the discrete incompressibility condition, guaranteeing exact conservation of the fluid volume, with the aid of markers. In the subsequent arguments and numerical calculations we use the condition

$$V_{j+1/2} = V^0_{j+1/2} = \text{const}. \tag{1.3}$$

Here $V_{j+1/2}$ is the volume that is cut from the fluid layer by the vertical lines drawn from S_j and S_{j+1} (see Fig. 1). It is clear that in principle other partitioning techniques are also possible. The relations (1.3) are holonomic constraints, therefore the Lagrangian of the examined system takes the form

$$L = T - \Pi + \sum_s \lambda_{s+1/2}\,(V_{s+1/2} - V^0_{s+1/2}), \tag{1.4}$$

where $\lambda_{s+1/2}$ are the Lagrange multipliers.

Here the degrees of freedom are ξ_i, σ_i, x_i, y_i, therefore it is necessary to further introduce some closing relations, connecting the motion of the markers with the averaged motion of the fluid. We use as these relations the nonholonomic constraints of the form

$$\delta x_i = \delta\xi_i \cos\varphi_i - \delta\sigma_i \sin\varphi_i, \quad \delta y_i = \delta\xi_i \sin\varphi_i + \delta\sigma_i \cos\varphi_i \tag{1.5}$$

(φ_i is the slope of the tangent to the bottom at the point x_i). Let d(x) denote the undisturbed fluid depth, then $\tan\varphi_i = -d_x(x_i)$. The constraints (1.5) postulate that the markers move as liquid particles on the free boundary with account for the shallow-water approximation.

The relations (1.1)-(1.5) completely define the motion of the system. Selecting $\delta\xi_i$ and $\delta\sigma_i$ as the independent variations, we easily obtain from the Hamilton principle the following Lagrange equations:

$$\begin{gathered} m_i\ddot{\xi}_i = \frac{\partial F}{\partial x_i}\cos\varphi_i + \frac{\partial F}{\partial y_i}\sin\varphi_i, \\ \alpha m_i\ddot{\sigma}_i = -\frac{\partial F}{\partial x_i}\sin\varphi_i + \frac{\partial F}{\partial y_i}\cos\varphi_i, \\ F = \sum_s \lambda_{s+1/2} V_{s+1/2} - \Pi, \quad \dot{x}_i = u_i = \dot{\xi}_i\cos\varphi_i - \dot{\sigma}_i\sin\varphi_i, \\ \dot{y}_i = v_i = \dot{\xi}_i\sin\varphi_i + \dot{\sigma}_i\cos\varphi_i, \quad V_{s+1/2} = V^0_{s+1/2}. \end{gathered} \tag{1.6}$$

We shall present some other formulas. If we select the Cartesian coordinate system so that $y = 0$ corresponds to the undisturbed free surface, then we have for the general position marker

$$\frac{\partial \Pi}{\partial x_k} = \frac{\rho g}{6}(y_{k-1} - y_{k+1})(y_{k-1} + y_k + y_{k+1}),$$

$$\frac{\partial \Pi}{\partial y_k} = \frac{\rho g}{6}[(x_{k+1} - x_{k-1})(y_{k-1} + 2y_k) + (x_{k+1} - x_k)(y_{k+1} - y_{k-1})], \tag{1.7}$$

$$V_{s+1/2} = \frac{1}{2}(x_{s+1} - x_s)(y_s + d(x_s) + y_{s+1} + d(x_{s+1})).$$

By virtue of the known theorems of classical mechanics, the system (1.6) exhibits the total energy conservation law, and for the case of a smooth bottom in the absence of side walls or for the case of a localized disturbance it also exhibits the law of conservation of the horizontal component of the momentum.

For the system (1.6), similarly to the contiuum case, we can study the dispersion of linear harmonic surface waves in an infinite fluid layer of depth d = const. We introduce dimensionless variables with the aid of the length scale d and the velocity scale $U = \sqrt{gd}$ and distribute the particles on the surface of the undisturbed layer uniformly with the dimensionless spacing h. Then, linearizing (1.6) and (1.7) in the vicinity of the state of rest, we can obtain the following exact law of dispersion of the linear waves:

$$\omega^2 = \frac{2 + \cos kh}{3} \frac{4 \operatorname{tg}^2 \frac{kh}{2}}{4\alpha \operatorname{tg}^2 \frac{kh}{2} + h^2} \tag{1.8}$$

(ω and k are the dimensionless wave frequency and wavenumber). In the limit as $h \to 0$

$$\omega^2 = \frac{k^2}{1 + \alpha k^2}. \tag{1.9}$$

For $\alpha = 1/3$ the expression (1.9) is the known dispersion relation, characteristic for many nonlinear-dispersion shallow-water models. By slightly varying α in the vicinity of the value 1/3, we can obtain from (1.8) in a certain wavenumber interval an even better approximation of the exact dispersion law for linear waves $\omega^2 = k\tanh(kh)$. Figure 2 shows two dispersion curves (1.8) with h = 0.3 (curves 2 and 4 for $\alpha = 0.27$ and 1/3) in comparison with the exact law (curve 1) and the law (1.9) with $\alpha = 1/3$ (curve 3). The wavenumber interval is selected so that the shortest waves have a dimensionless length $\lambda = 2\pi/k = 3$, in this case 10 cells of the discrete model grid correspond to one length of this wave. We see that the selection $\alpha = 0.27$ yields a far better approximation of the exact law than (1.9) with $\alpha = 1/3$. We note that reduction of α relative to 1/3 for the short waves is physically justified, since in these waves the vertical velocity decreases faster with depth than a linear function.

We shall now show how the equations (1.6), (1.7) themselves transform as $h \to 0$. For simplicity we shall examine the case d(x) = const, then $\varphi_i = 0$, $x_i = \xi_i$, $y_i = \sigma_i$. We shall consider that in the state of rest all the particles are distributed uniformly with the spacing h, i.e., all the m_i are the same and equal to $m_i = hd$. We introduce the Lagrangian coordinate of the particles q, where $q_i = ih$, and also the total depth H = y + d. Differentiating the constraints (1.3) with respect to time and considering (1.7), we obtain

$$(y_i + y_{i+1} + 2d)(u_{i+1} - u_i) + (x_{i+1} - x_i)(v_{i+1} + v_i) = 0. \tag{1.10}$$

As $h \to 0$ we have, respectively, from (1.3) and (1.10)

$$\frac{\partial x}{\partial q} = \frac{d}{H}; \tag{1.11}$$

$$H\frac{\partial u}{\partial q} + v\frac{\partial x}{\partial q} = 0. \tag{1.12}$$

The first two equations (1.6) yield in the limit

$$d\dot{u} = -\frac{\partial}{\partial q}\lambda H + qy\frac{\partial y}{\partial q}; \tag{1.13}$$

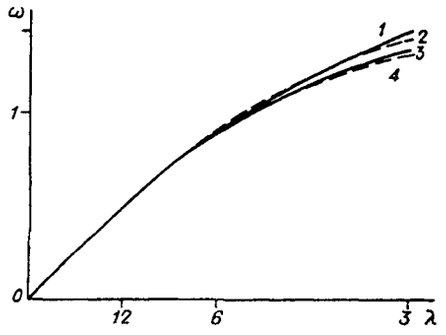

Fig. 2

$$\alpha d\dot{v} = \lambda \frac{\partial x}{\partial q} - gy \frac{\partial x}{\partial q}. \tag{1.14}$$

Introducing, as usual, the free surface vertical rise function $\eta(t, x(t, q)) = y(t, q)$ and considering that the total derivative with respect to time $D\eta = \dot{\eta} = \eta_t + u\eta_x = v$, we finally obtain from (1.11)-(1.14)

$$\begin{gathered} \eta_t + (Hu)_x = 0, \\ Du + g\eta_x = -\frac{\alpha}{H}(H^2 D^2 \eta)_x. \end{gathered} \tag{1.15}$$

The system (1.15) with $\alpha = 1/3$ is the well-known nonlinear-dispersion shallow-water model for waves of finite amplitude [5]. It was presented in this form in [6]. Thus, in the case of a smooth bottom and with $\alpha = 1/3$ the discrete model formulated above actually is a fully conservative difference scheme in Lagrangian coordinates for the equations that are equivalent to those of [5]. The derivation of these equations presented above is simpler. However, if our objective is numerical modeling, then formulation of the fully conservative scheme for the equations in the form (1.15) is not a trivial problem. We further note that the sequence that is usual for numerical modeling is run through here in the reverse direction, i.e., we first derived the discrete numerical model and only then the corresponding continuum model.

In the case of a nonsmooth bottom for a sufficiently smooth depth function d(x) the limiting equations can be reduced to the analogous form

$$\begin{gathered} \eta_t + (Hu)_x = 0, \\ Du + g\eta_x = -\frac{\alpha}{H}(H^2 (A + B))_x + \alpha A d_x + B(1 + \alpha d_x), \end{gathered} \tag{1.16}$$

where $A = D^2\eta$; $B = Dd_x/(1 + d_x^2)$; the dispersion term in the right side of the second equation (1.16) now differs from that presented in [5, 6]. We note that the basic premises also differ here, since in [5] even in the nonsmooth bottom case it is assumed that the horizontal velocity u is independent of y. We further note that in the discrete model (1.6), in contrast with the equations (1.16), the formal requirements on smoothness of the depth function d(x) are significantly weaker; specifically, infinite or very large accelerations do not arise if the bottom has a break or a segment with small radius of curvature, as, for example, in the wave runup problem examined below.

We should also say a few words about the points of free surface contact with rigid walls. The markers are also such points, i.e., they serve as the nodes of the broken line approximating the free boundary. In contrast with the other particles, they can travel only along the rigid wall, i.e., they have a single degree of freedom ξ_i. Therefore in (1.6) there are no equations for them in the direction σ_i. The expressions for the derivatives of Π change somewhat for these particles. Thus, in the problem examined below of wave runup onto a shallow slope we have for the extreme marker with the number N, describing the motion of the "cutoff" point, we have

$$\frac{\partial \Pi}{\partial x_N} = \frac{\rho g}{6}(y_{N-1} - y_N)(y_{N-1} + 2y_N), \quad \frac{\partial \Pi}{\partial y_N} = \frac{\rho g}{6}(x_N - x_{N-1})(y_{N-1} + 2y_N).$$

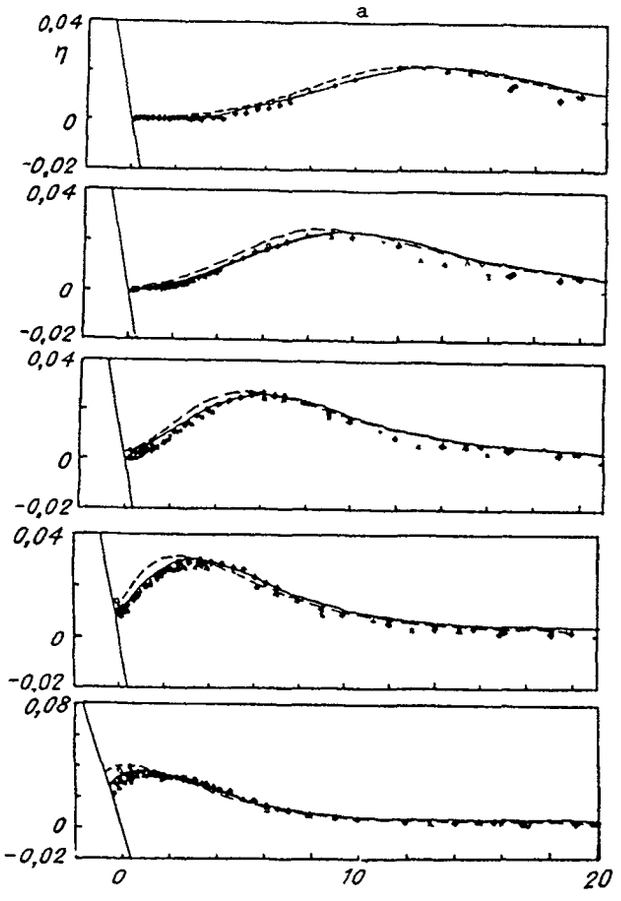

Fig. 3

These expressions can be obtained both directly from (1.2) and also from (1.7), if we introduce a fictitious particle with the number N + 1 and set by definition $x_{N+1} = x_N$, $y_{N+1} = y_N$.

2. Numerical Calculations. For the numerical solution of the system (1.6) we used the algorithm of [7], developed specifically for the discrete incompressible fluid models. As usual, in solving the nonlinear-dispersion shallow-water equations it becomes necessary to invert at each step in time an elliptic operator. Here this elliptic problem is the system of linear equations for finding at each step the Lagrange multipliers [7]. It is easy to show that for the given model the matrix of this system is tridiagonal, symmetric, and positive-definite. A marching procedure was used for its inversion. It is also not difficult to show that the numerical algorithm that we used is equivalent with respect to the number of calculations to the simple explicit system for the equations (1.15), (1.16) in Lagrangian coordinates.

All the calculations were made for $d_0 = 1$, $g = 1$, $\rho = 1$, which corresponds to nondimensionalization of the variables with the aid of the scales d_0, $\sqrt{gd_0}$ and ρ. The numerical experiments showed first of all that the described discrete model has even on a quite coarse mesh has solutions in the form of solitary waves, which by virtue of the conservative properties of the model and the numerical algorithm propagate along the smooth bottom with constant mean velocity, amplitude, and energy. For $\alpha = 1/3$ these solutions were compared with the classical Rayleigh solitons

$$\eta = a \operatorname{sech}^2 \left[(x - x_0) \sqrt{\frac{3a}{4(a+1)}} \right]. \tag{1.17}$$

Thus, for the soliton with amplitude $a = 0.7$ with values of the steps in space $h = 1$ and in time $\tau = 0.5$ the maximal relative deviation of the numerical solution from (1.17) did not exceed, respectively, for the shape of the soliton and its phase velocity

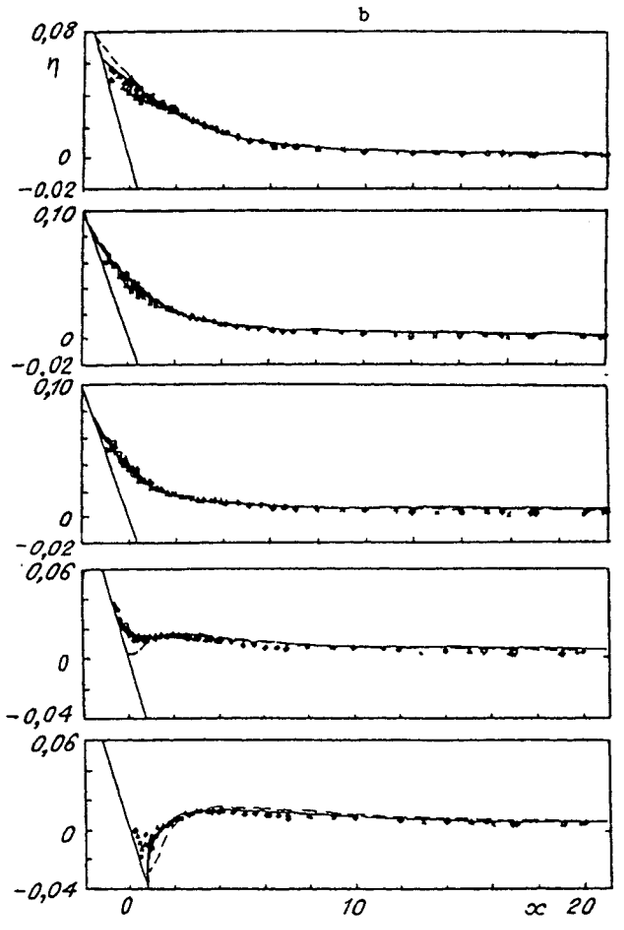

Fig. 3 (continued)

1 and 0.3%. For h = 0.5 and τ = 0.25 the deviation decreased to 0.2 and 0.09%. The oscillations of the wave total energy relative to the constant average value did not exceed, respectively, 0.005 and 0.003%, i.e., they were very close to the roundoff errors. These calculations were carried out to values of the dimensionless time t = 400 or more.

The next test was a comparison of the solitary wave runup calculations with the results of [8-10]. In the calculations presented below the bottom slope φ_i near the breakpoint was calculated with the aid of averaging over three neighboring particles, although in principle this procedure is not mandatory and exerts some smoothing influence on the form of the free boundary only for large slopes. Figure 3 presents a series of pictures, demonstrating the runup of a solitary wave of amplitude a = 0.019 onto a gentle slope with cotangent of the inclination angle 19.85. The free surface vertical rise profiles were derived with an interval Δt = 5. The results of the numerical calculations using the discrete model (solid curve) are compared with the experimental points and with the approximate solution of the shallow-water equations (dashed curves) from [8].

Figure 4 presents for this problem the calculated (dashed curves) time dependences of the free surface vertical rise at four fixed points on the sloping bank in comparison with the data of [8] (solid curves — experiment, dotted curves — theory). The calculations using the discrete model were made with α = 1/3 and τ = 0.2, the value of h varied from 1 on the smooth bottom to 0.2 near the "cutoff" point. The comparison shows that the discrete model, having because of account for dispersion a significantly broader region of applicability than the conventional shallow-water equations, in the present problem, where the dispersion effects are not significant, works no more poorly and describes quite well the runup process with the use of a quite coarse computational mesh.

Figure 5 presents successive pictures of the runup of a wave with large amplitude (a = 0.19) onto a slope with an angle of 30°. Here the calculated data (dashed lines) are compared with experimental data (solid lines) from [9]. The pictures are presented with a time interval Δt = 2.86.

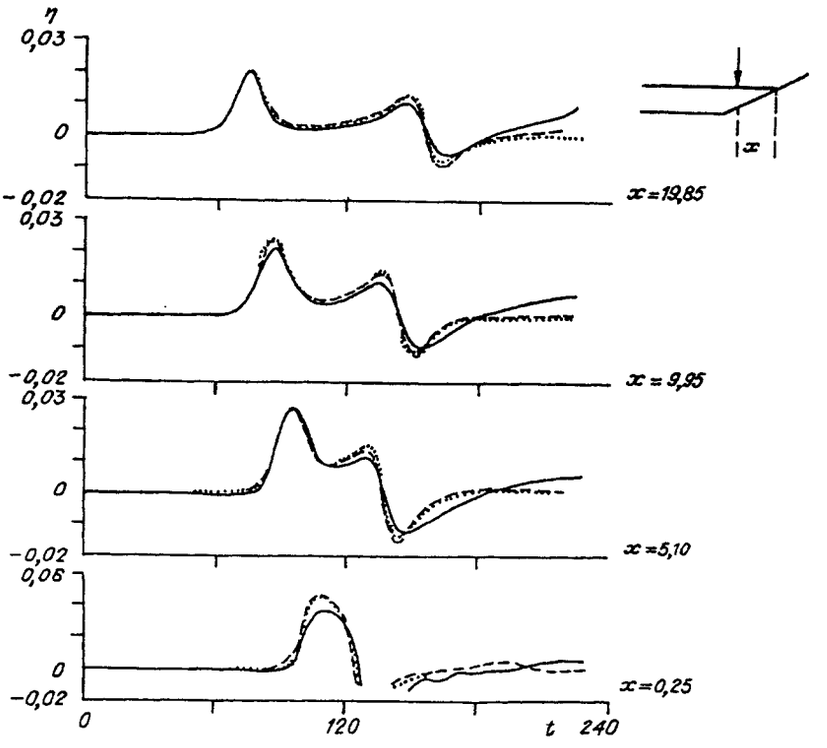

Fig. 4

TABLE 1

$ctg\theta$ (θ, deg)	A	Maximal runup		
		numerical and asymptotic solutions [4, 8-10] (min-max)	experiment [8, 9]	discrete shallow-water model
10,000	0,030	0,100—0,112	—	0,117
(5,7)	0,050	0,180—0,212	—	0,217 (0,215)
3,732	0,050	0,129—0,135	0,173	0,139
	0,100	0,308—0,308	0,281	0,309
(15)	0,200	0,732—0,766	0,599	0,684 (0,687)
3,333	0,050	0,122—0,150	0,121	0,134
(16,7)	0,100	0,291—0,310	0,264	0,298 (0,295)
2,747	0,050	0,111—0,127	0,115	0,125
	0,098	0,257—0,275	0,252	0,267
(20)	0,193	0,599—0,600	0,552	0,567
	0,294	0,958—1,016	0,898	0,920 (0,926)
2,000	0,113	0,27	0,284	0,278
	0,195	0,49	0,526	0,497
(26,6)	0,29	0,79	0,825	0,774
	0,41	1,17	1,220	1,142
	0,50	1,49	1,530	1,416 (1,422)
1,000	0,060	0,125—0,129	0,115	0,125
	0,113	0,24	—	0,236
	0,100	0,159—0,216	0,212	0,209
(45)	0,195	0,44	—	0,395
	0,200	0,451—0,504	0,454	0,404
	0,29	0,70	—	0,574
	0,41	1,03	—	0,795
	0,480	1,249—1,610	1,270	0,916
	0,50	1,30	—	0,951 (0,953)

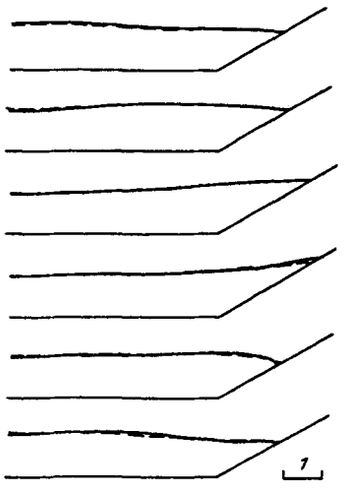

Fig. 5

Finally, Table 1 summarizes the results of the numerical calculations and laboratory experiments of various authors with regard to maximal runup of solitary waves onto an inclined wall in the range of amplitudes from 0.03 to 0.5 and cotangents of the inclination angles from 1 to 10, taken from [4, 8-10]. Also shown here are the results of calculations using the discrete model for the same values of α, τ, and h as above. The magnitudes of the runup for values of τ and h that are half as large are shown in parentheses for comparison. We see that the theoretical results that are available for this problem differ markedly from one another. The scatter of the calculated values sometimes reaches 20% or more. If we consider the experimental results, then the scatter increases still more. As a rule, the results of the calculations using the discrete model lie well within this range, except for the cases of waves of large amplitude for steep slopes, particularly for $\theta = 45°$. The latter is quite understandable, since the assumptions made in the derivation of the model concerning the distribution of the velocities with regard to depth are physically justified, strictly speaking, only for $|d_x| \ll 1$. The calculations show that the magnitude of the runup in this problem is actually described quite well for $|d_x| \leq 1/2$.

The drawbacks of the described model include the upper limit on the spatial step h, following from the dispersion relation (1.8). It is easy to see that for the shortest numerical harmonics with wavelength $\lambda = 2h$ the phase velocity $c^2 = (\omega^2/k^2) = (h^2/3\pi^2\alpha)$ increases without limit with increase of h. For $h > \pi\sqrt{3\alpha}$ this leads to qualitative change of the dispersion law, when the phase velocity has a maximum that is greater than unity in the short-wave region. Because of this, for such values of h the shape of the long waves is distorted, for example the shape of the solitons of very small amplitude, for which the selection of a coarse step would seem to be quite acceptable from similarity considerations.

REFERENCES

1. V. A. Korobitsyn and Z. E. Libin, "On a numerical method for solving unsteady problems of an incompressible fluid with a free surface," in: Dynamics of Elastic and Rigid Bodies, Interacting with a Liquid [in Russian], Tomsk Univ., Tomsk (1975).
2. V. M. Goloviznin, A. A. Samarskii, and A. P. Favorskii, "Variational approach to the construction of finite-difference models in hydrodynamics," DAN SSSR, **235**, No. 6, 1285-1288 (1977).
3. J. M. Augenbaum, "A Lagrangian method for the shallow water equations based on a Voronoi mesh — Flows on a rotating sphere," Lecture Notes in Physics, Berlin et al., **238**, 54-86, Springer-Verlag (1985).
4. A. M. Frank, "Numerical modeling of solitary surface waves in the framework of the discrete incompressible fluid model," Zh. Prikl. Mekh. Tekh. Fiz., No. 3, 95-101 (1989).
5. A. E. Green and P. M. Naghdi, "A derivation of the equations for wave propagation in water of variable depth," J. Fluid Mechanics, **78**, 237-246 (1976).

6. R. S. Ertekin, W. C. Webster, and J. V. Wehausen, "Waves caused by a moving disturbance in a shallow channel of finite width," J. Fluid Mechanics, **169**, 275-292 (1986).
7. A. M. Frank, "Fully conservative numerical algorithm for discrete incompressible fluid models," in: Modeling in Mechanics [in Russian], **1(18)**, No. 5, 134-144, Vts SO AN SSSR; ITPM SO AN SSSR (1987).
8. C. E. Synolakis, "The runup of solitary waves," J. Fluid Mechanics, **185**, 523-545 (1987).
9. G. Pedersen and B. Gjevik, "Run-up of solitary waves," J. Fluid Mechanics, **135**, pp. 283-290 (1983).
10. N. V. Novikova and G. S. Khakimzyanov, "On the numerical calculation of potential ideal incompressible fluid flows with a free boundary," Deposited in VINITI May 8, 1990. No. 2451-B90, Moscow (1990).